Drevets WC (2000) Functional anatomical abnormalities in limbic and prefrontal cortical structures in major depression. Prog Brain Res 126:413–431.

Drevets WC (2001) Neuroimaging and neuropathological studies of depression: implications for the cognitive-emotional features of mood disorders. Curr Opin Neurobiol 11:240–249.

Duric V, Banasr M, Licznerski P, Schmidt HD, Stockmeier CA, Simen AA et al. (2010) A negative regulator of MAP kinase causes depressive behavior. Nat Med 16:1328–1332.

Ermisch A, Rühle HJ, Landgraf R, Hess J (1985) Blood–brain barrier and peptides. J Cereb Blood Flow Metab 5:350–357.

Fagioli S, Rossi-Arnaud C, Ammassari-Teule M (1991) Open field behaviours and spatial learning performance in C57BL/6 mice: early stage effects of chronic GM1 ganglioside administration. Psychopharmacology (Berl) 105:209–212.

Francis SH, Corbin JD (2005) Sildenafil: efficacy, safety, tolerability and mechanism of action in treating erectile dysfunction. Expert Opin Drug Metab Toxicol 1:283–293.

Frasch A, Zetzsche T, Steiger A, Jirikowski GF (1995) Reduction of plasma oxytocin levels in patients suffering from major depression. Adv Exp Med Biol 395:257–258.

Gainer H, Wray S (1994) Lactation and its hormonal control. In: The physiology of reproduction (Knobil E, Neill JD, eds), pp 1099–1129. New York: Raven Press.

Ghasemi M, Sadeghipour H, Mosleh A, Sadeghipour HR, Mani AR, Dehpour AR (2008) Nitric oxide involvement in the antidepressant-like effects of acute lithium administration in the mouse forced swimming test. Eur Neuropsychopharmacol 18:323–332.

Gourley SL, Wu FJ, Kiraly DD, Ploski JE, Kedves AT, Duman RS et al. (2008) Regionally specific regulation of ERK MAP kinase in a model of antidepressant-sensitive chronic depression. Biol Psychiatry 63:353–359.

Harrison WM, Rabkin JG, Ehrhardt AA, Stewart JW, McGrath PJ, Ross D et al. (1986) Effects of antidepressant medication on sexual function: a controlled study. J Clin Psychopharmacol 6:144–149.

Harvey BH (1996) Affective disorders and nitric oxide: a role in pathways to relapse and refractoriness? Hum Psychopharmacol 11:309–319.

Insel TR, Shapiro LE (1992) Oxytocin receptor distribution reflects social organization in monogamous and polygamous voles. Proc Natl Acad Sci U S A 89:5981–5985.

Jesse CR, Bortolatto CF, Savegnago L, Rocha JB, Nogueira CW (2008) Involvement of L-arginine-nitric oxide-cyclic guanosine monophosphate pathway in the antidepressant-like effect of tramadol in the rat forced swimming test. Prog Neuropsychopharmacol Biol Psychiatry 32:1838–1843.

Liebenberg N, Harvey BH, Brand L, Brink CB (2010a) Antidepressant-like properties of phosphodiesterase type 5 inhibitors and cholinergic dependency in a genetic rat model of depression. Behav Pharmacol 21:540–547.

Liebenberg N, Müller HK, Fischer CW, Harvey BH, Brink CB, Elfving B, Wegener G (2011) An inhibitor of cAMP-dependent protein kinase induces behavioural and neurological antidepressant-like effects in rats. Neurosci Lett 498:158–161.

Liebenberg N, Wegener G, Harvey BH, Brink CB (2010b) Investigating the role of protein kinase-G in the antidepressant-like response of sildenafil in combination with muscarinic acetylcholine receptor antagonism. Behav Brain Res 209:137–141.

Matsushita H, Tomizawa K, Okimoto N, Nishiki T, Ohmori I, Matsui H (2010) Oxytocin mediates the antidepressant effects of mating behavior in male mice. Neurosci Res 68:151–153.

McEwen BS (1999) Stress and hippocampal plasticity. Annu Rev Neurosci 22:105–122.

Montejo AL, Llorca G, Izquierdo JA, Rico-Villademoros F (2001) Incidence of sexual dysfunction associated with antidepressant agents: a prospective multicenter study of 1022 outpatients. J Clin Psychiatry 62:10–21.

Neumann ID (2001) Alterations in behavioral and neuroendocrine stress coping strategies in pregnant, parturient and lactating rats. Prog Brain Res 133:143–152.

Neumann ID (2008) Brain oxytocin: a key regulator of emotional and social behaviors in both females and males. J Neuroendocrinol 20:858–865.

Numan M, Insel TR (2003) Hormonal and nonhormonal basis of maternal behavior. In: The neurobiology of parental behavior (Numan M, Insel TR, eds), pp 8–41. New Jersey: Springer.

Nurnberg HG, Hensley PL, Gelenberg AJ, Fava M, Lauriello J, Paine S (2003) Treatment of antidepressant-associated sexual dysfunction with sildenafil: a randomized controlled trial. JAMA 289:56–64.

Ozsoy S, Esel E, Kula M (2009) Serum oxytocin levels in patients with depression and the effects of gender and antidepressant treatment. Psychiatry Res 169:249–252.

Puzzo D, Sapienza S, Arancio O, Palmeri A (2008) Role of phosphodiesterase 5 in synaptic plasticity and memory. Neuropsychiatr Dis Treat 4:371–387.

Ring RH, Schechter LE, Leonard SK, Dwyer JM, Platt BJ, Graf R et al. (2010) Receptor and behavioral pharmacology of WAY-267464, a non-peptide oxytocin receptor agonist. Neuropharmacology 58:69–77.

Scantamburlo G, Hansenne M, Fuchs S, Pitchot W, Maréchal P, Pequeux C et al. (2007) Plasma oxytocin levels and anxiety in patients with major depression. Psychoneuroendocrinology 32:407–410.

Sheline YI, Gado MH, Kraemer HC (2003) Untreated depression and hippocampal volume loss. Am J Psychiatry 160:1516–1518.

Sheline YI, Wang PW, Gado MH, Csernansky JG, Vannier MW (1996) Hippocampal atrophy in recurrent major depression. Proc Natl Acad Sci U S A 93:3908–3913.

Shin MS, Ko IG, Sung YH, Kim SE, Kim BK, Kim CJ et al. (2010) Vardenafil enhances oxytocin expression in the paraventricular nucleus without sexual stimulation. Int Neurourol J 14:213–219.

Slattery DA, Neumann ID (2010) Oxytocin and major depressive disorder: experimental and clinical evidence for links to a etiology and possible treatment. Pharmaceuticals 3:702–724.

Stockmeier CA, Mahajan GJ, Konick LC, Overholser JC, Jurjus GJ, Meltzer HY et al. (2004) Cellular changes in the postmortem hippocampus in major depression. Biol Psychiatry 56:640–650.

Tomizawa K, Iga N, Lu YF, Moriwaki A, Matsushita M, Li ST et al. (2003) Oxytocin improves long-lasting spatial memory during motherhood through MAP kinase cascade. Nat Neurosci 6:384–390.

Weisstaub NV, Zhou M, Lira A, Lambe E, González-Maeso J, Hornung JP et al. (2006) Cortical 5-HT_{2A} receptor signaling modulates anxiety-like behaviors in mice. Science 313:536–540.

Zetzsche T, Frasch A, Jirikowski GF, Murck H, Steiger A (1996) Nocturnal oxytocin secretion is reduced in major depression. Biol Psychiatry 39:584.

Zhang L, Zhang Z, Zhang RL, Cui Y, LaPointe MC, Silver B et al. (2006a) Tadalafil, a long-acting type 5 phosphodiesterase isoenzyme inhibitor, improves neurological functional recovery in a rat model of embolic stroke. Brain Res 1118:192–198.

Zhang R, Wang Y, Zhang L, Zhang Z, Tsang W, Lu M et al. (2002) Sildenafil (Viagra) induces neurogenesis and promotes functional recovery after stroke in rats. Stroke 33:2675–2680.

Zhang RL, Zhang Z, Zhang L, Wang Y, Zhang C, Chopp M (2006b) Delayed treatment with sildenafil enhances neurogenesis and improves functional recovery in aged rats after focal cerebral ischemia. J Neurosci Res 83:1213–1219.

Zhang Z, Klyachko V, Jackson MB (2007) Blockade of phosphodiesterase type 5 enhances rat neurohypophysial excitability and electrically evoked oxytocin release. J Physiol 584:137–147.

Zomkowski AD, Engel D, Gabilan NH, Rodrigues AL (2010) Involvement of NMDA receptors and L-arginine-nitric oxide-cyclic guanosine monophosphate pathway in the antidepressant-like effects of escitalopram in the forced swimming test. Eur Neuropsychopharmacol 20:793–801.

(Accepted 1 November 2011)
(Available online 09 November 2011)

Current Organ Topics:

Central Nervous System Tumor
脳腫瘍
中枢神経系原発悪性リンパ腫

Ⅰ．中枢神経系原発悪性リンパ腫の標準治療と問題点

森　鑑二，有田　憲生
（兵庫医科大学　脳神経外科）

〔*Jpn J Cancer Chemother* 39(6): 888-891, *June*, 2012〕

はじめに

中枢神経系原発悪性リンパ腫（PCNSL）は，中枢神経系外に病巣をもたないリンパ球由来の悪性腫瘍で，わが国では原発性脳腫瘍のうち約3%程度を占めている[1]。本来リンパ系を有しない神経系で原発する理由は不明であるが，高齢者の発生頻度が高く，近年増加している腫瘍の一つである。組織学的には95%以上がびまん性大型B細胞性リンパ腫（DLBL）であるため，本稿ではPCNSLのうちDLBLに対する標準治療について述べる。本腫瘍は放射線感受性が高い腫瘍であるが，放射線単独療法では生存期間中央値が約12か月で，5年生存率が約18%という報告がなされ，奏効率は高いものの，長期間の抗腫瘍効果が低いことが示されている[2]。また，全身性節外性DLBLの標準的治療法であるCHOP（D）療法（サイクロフォスファミド/ドキソルビシン/ビンクリスチン/デキサメサゾン）と全脳への放射線照射との併用療法も，生存期間中央値が16か月と有意な上乗せ効果が確認できなかった[3]。これは主に，サイクロフォスファミド，ドキソルビシンが脳血液関門を通過しない薬剤であることが原因と考えられている。これに対して1990年代以降，大量のメソトレキサートを急速に点滴静注し，これと他の薬剤や放射線治療を併用することで，放射線照射単独療法と比較して無増悪生存期間と全生存期間が延長できることが明らかになった。高い血中濃度を得ることによって脳血液関門を通過させることができるようになり，またロイコボリンの投与にて正常細胞を救援することで，神経系への毒性を抑えたまま抗腫瘍効果を高められると考えられている。その後，メソトレキサートを上回る効果を示した抗腫瘍薬や代替療法が出現していないため，現時点では大量メソトレキサートを中心とした化学療法と全脳放射線照射の併用が事実上の標準治療となっている。

1．PCNSLの標準治療

大量メソトレキサート/ロイコボリン救援療法（HD-MTX）を中心とした化学療法＋全脳放射線照射は標準治療であると同時に，エビデンスを備えているといえる唯一の治療法でもある。米国のNational Comprehensive Cancer Network（NCCN）や英国のBritish Committee for Standards in Haematology（BCSH）のガイドラインでは，初発症例に対する治療として推奨されている。これまでに報告された前向きで症例数が25例以上の治療について主なものを表1に示す[4-22]。メソトレキサートは3 g/m^{2}以上用いられることが多く，2～3週間間隔で繰り返されている。これらの治療では，奏効率，著効率は化学療法後でそれぞれ72～94%と18～67%，放射線治療追加後にはそれぞれ68～94%と33～87%に達している。2年生存率と5年生存率はそれぞれ50～75%，26～51%で初期治療が奏効する割合は高いといえるものの，効果の乏しい症例や無効例が少なからず存在することと，長期生存の割合も高いとはいえないこともわかる。本邦における多数例の報告には，Hiragaらの報告[23]とPCNSL研究会による多施設第Ⅱ相試験の報告[24]がある。前者では，3.5 g/m^{2}のメソトレキサートを3時間で急速点滴静注した群と，6時間で点滴静注した群を比較し，3時間点滴静注群のほうが6時間点滴静注群よりも髄液中への薬剤移行が有意に促進されること，腫瘍縮小効果も有意に高くなることが報告された。また，2群間で有意差はみられなかったが，3時間点滴静注群の無増悪生存期間と生存期間の中央値は，メソトレキサート単独＋放射線照射で50か月と60か月以上という成績であった。後者では，3.5 g/m^{2}でのHD-MTXを2週間間隔で3コース行い，30～40 Gyの全脳照射を加えるというプロトコールが用いられた。中間報告では，放射線治療追加群55例における奏効率85%，生存期間中央値が44か月とされている。臨床試験では，年齢に上限が定められていることも少なくないため，非高齢者で比較的performance status（PS）のよい症例に対する標準治療の成績は奏効率80%，CR達成率70%程度で，全生存期間の中央値3～4年程度といえよう。メソトレキサートの量，コース数，各コース間の間隔などについてはまだ

表1

症例数	初期治療 療法	使用薬剤	Mの投与量	全奏効率（%）	著効例（%）	観察期間 中央値（月）	生存率（%） 2年	5年	神経毒性（%）
化学療法のみ									
31[5]	化療単独	M	8 g/m²/14 d	100	NR	31	63	NR	0
25[6]	化療単独	M	8 g/m²/14 d	74	52	23	70	NR	5
65[7]	化療単独	M＋VICA	5 g/m²/28 d	71	61	26	69	43	3
37[8]	化療単独	M	8 g/m²/14 d	35	30	56	51	25	20
HD-M単剤＋放射線治療									
25[9]	化療＋放	M	3.5 g/m²/21 d	88-92	56-88	60	58	38	8
46[10]	化療＋放	M	1 g/m²/7 d	NR-95	NR-82	36	62	37	22
31[11]	化療＋放→化療	M	1 g/m²/7 d	64-87	NR-87	97	72	22	32
HD-Mを含む多剤併用＋放射線治療									
25[12]	化療＋放	AaCMOP	3 g/m²/21 d	72-72	67-78	24	70	58	0
57[13]	化療＋放→化療	ABnMO±CHOP	1.5-3 g/m²/14 d	68-71	62-64	59	60	36	NS
56[14]	化療＋放	BnMNP	1.5 g/m²/28 d	71-100	53-61	8	86	NS	29
31[15]	化療＋放	ABCMOP	2 g/m²/15 d	89-67		24	48	36	7
52[16]	化療＋放→化療	MNO	3.5 g/m²/7 d	90-94	56-87	60	75	40	25
102[17]	化療＋放	MNO	2.5 g/m²/14 d	94-NR	58-NR	56	64	32	15
52[18]	化療＋放	BnMOP	3 g/m²/14 d	NR-81	33-69	27	69	NR	12
41[19]	化療＋放	AIMT	3.5 g/m²/21 d	76-83	44-56	49	50	41	NR
30[20]	化療＋放→化療	MNOR	3.5 g/m²/14 d	93-NR	44-77	37	67	NR	NR
無作為化試験									
79[21]	化療＋放	M	3.5 g/m²/21 d	40-40	18-30	30	39	26	20
		Ma	3.5 g/m²/21 d	69-74	46-64		56	48	6
551[22]	化療±放	M or Ml	4 g/m²/14 d	54-NR	35-80（＋放）	50.7	60	32	49
				65	42			26	

NR: not reported，化療: 化学療法，放: 放射線療法，→化療: 化学療法後放射線治療を行いさらに化学療法追加，d: day
初期治療に使用された薬剤: Aもしくは B: アドリアマイシン，a: シタラビン，B: ブレオマイシン，Bn: BCNU，C: サイクロフォスファミド，E: エトポシド，HD-M: 大量メソトレキサート，I: イフォスファマイド，M: メソトレキサート，N: プロカルバジン，O: ビンクリスチン，P: プレドニゾロン，R: リツキシマブ，T: チオテパ，Te: テモゾロミド，V: テニポシド

標準化がなされていない。これらの臨床試験では年齢の上限が定められていたり，PSの悪い症例は除外されていることが多く，70歳以上の高齢者の占める割合が高く，PSの悪い症例も多い臨床現場に適応する際には考慮が必要と考える。

2．標準治療における問題点と対策

現在，本疾患は標準治療後，著効例であっても再発はほぼ避けられない。一方，再発時の治療法は確立していない。同様にHD-MTXの効果が低い，あるいは抵抗性の症例に対する治療法も同様である。さらに，高齢者においてことに問題になる放射線治療後の遅発性神経毒性の問題も無視できない。

化学療法の治療強度を高める試みは，放射線障害を回避するために化学療法単独での治療成績改善を目的として計画されることが多く，メソトレキサートを増量する単独療法，多剤併用療法，超大量の化学療法に造血幹細胞移植を併用する方法が主なアプローチである。増量したメソトレキサート単剤療法では8 g/m²を用いた報告が多く，その一つであるNABTT 96-07で，6.5年以上観察した長期成績が2008年に報告された。著効例12例のうち，5例が中央値6.8年間，無再発で経過している[35]。生存期間の中央値は55.4か月であったが，原疾患死に関しては72か月でも中央値に到達していない。観察期間が約2年の時点での報告では23例中12例(52%)がCRで，全奏効率は72%，無増悪生存期間の中央値は12.8か月であった[6]。増量したメソトレキサート単剤投与ではgrade 3，4の有害事象は少なく，安全に実施できるとされる。一方で，放射線治療を追加しなければ，著効例でも比較的早期に再発するという傾向が指摘されている[36]。

HD-MTXを中心とし，様々な薬剤を併用した多剤併用療法も試みられている。最近，二つの無作為化試験の

結果が報告された。HD-MTX単独とそれに高用量のシタラビンを併用する群を比較した第Ⅱ相試験では，全奏効率が単独群40%（95% CI: 25-55），併用群69%（95% CI: 55-83）で（p=0.009），CR達成率も単独群18%（95% CI: 6-30），併用群46%（95% CI: 31-61）と，ともに有意差が認められた（p=0.006）。さらに，3年後の無増悪生存率についても単独群21%，併用群31%で有意差を認めているが（p=0.001，hazard ratio: 0.54，95% CI: 0.31-0.92），3年後の全生存率は単独群32%，併用群46%で有意差は得られなかった[25]。これらの点から，高用量のシタラビン併用は治療効果を高め，無再発生存期間を延長できると考えられた。また，本試験では放射線治療を全例に併用していたが，HD-MTXとイフォスファマイド併用群のHD-MTX単独に放射線治療を追加した群に対する全生存期間における非劣勢を検討したG-PCNSL-SG-1試験の結果が2010年に報告された[26]。全生存期間の中央値は放射線併用群では32.4か月（95% CI: 25.8-39.0），化学療法単独群では37.1か月（95% CI: 27.5-46.7）であり，両者間に有意差はみられなかったが，hazard ratio: 1.06（95% CI: 0.80-1.40，p=0.71）で仮説は証明されなかった。さらに，本試験では初期治療中の死亡率が13%であった。このように初期治療としての多剤併用療法はHD-MTX単独＋放射線治療に対して予後を改善できる可能性が示唆されるものの，その成績を大きく凌駕することはできていない。また，再発時などに多くの症例で放射線治療を行わざるを得ず，神経毒性の軽減という点でも課題が残されている。

化学療法を強化する方法のもう一つは，造血幹細胞移植併用大量化学療法である。2006年にIllerhausらは，65歳以下の症例に対して，8 g/m^{2}のHD-MTX後にカルムスチン，チオテパを用いて自家造血幹細胞移植併用大量化学療法を行った治療成績を報告している。登録症例30例中，幹細胞移植を併用した症例は23例で，5年後の生存率87%，全症例5年生存率は69%であったが，放射線治療群の24%で強い白質脳症が出現したと報告している[30]。彼らはさらに69歳以下を対象として，CR例には放射線治療を行わない方針で行われた研究の結果を2008年に報告しているが，ここでは観察期間の中央値25か月で，3年生存率は77%，良好な認知能が維持できているという[27]。このように，本療法には良好な治療成績を収めたものもあり，魅力的な方法ではあるが治療関連死が3%以上に上るなど，限られた症例に対して行われる研究段階の治療にとどまっているといえる[28]。

高齢者には高率に生じる，放射線治療による認知機能の低下も依然大きな問題である。65歳以上を対象として，3 g/m^{2}のMTX投与に放射線治療を延期させる方針で30例に行われた前向きの研究では，観察期間の中央値が78か月の時点での無増悪生存期間と生存期間の中央値はそれぞれ5.9か月と15.4か月であったが，8例が生存しており，3年後と5年後の生存率はともに33%であった[29]。心機能や腎機能が保たれていれば，HD-MTXは高齢者にも比較的安全に実施可能だが，容易に化学療法を強化できないため，治療成績改善のためには若年者とは異なるアプローチが必要である。テモゾロミドやリツキシマブの併用が報告され，高齢者の治療成績の改善が期待されている[30,31]。

おわりに

本疾患は希少癌腫のため，大規模な試験や無作為化試験の遂行が困難なこと，脳血液関門のために効果が得られる薬剤が限られるといった問題があり，他臓器の悪性腫瘍に比べ治療法の進歩が遅れているといわざるを得ない。しかしながら，リツキシマブの効果やラパチニブのような低分子薬品の登場を考慮すると，今後，中枢神経系外のDLBLに対する新規治療薬剤が本疾患の標準治療薬となる可能性があると期待してよいのではないだろうか。

文　献

1) The Committee of Brain Tumor Registry of Japan: Report of Brain Tumor Registry of Japan (1984-2000) 12th Edition. *Neurol Med Chir (Tokyo)* 49 (*Suppl*): 1-25, 2009.
2) Nelson DF, Martz KL, Bonner H, *et al*: Non-Hodgkin's lymphoma of the brain: can high dose, large volume radiation therapy improve survival? Report on a prospective trial by the Radiation Therapy Oncology Group (RTOG): RTOG 8315. *Int J Radiat Oncol Biol Phys* 23 (1): 9-17, 1992.
3) DeAngelis LM, Seiferheld W, Schold SC, *et al*: Combination chemotherapy and radiotherapy for primary central nervous system lymphoma: Radiation Therapy Oncology Group Study 93-10. *J Clin Oncol* 20 (24): 4643-4648, 2002.
4) Ferreri AJ: How I treat primary CNS lymphoma. *Blood* 118 (3): 510-522, 2011.
5) Guha-Thakurta N, Damek D, Pollack C, *et al*: Intravenous methotrexate as initial treatment for primary central nervous system lymphoma: response to therapy and quality of life of patients. *J Neurooncol* 43 (3): 259-268, 1999.
6) Batchelor T, Carson K, O'Neill A, *et al*: Treatment of primary CNS lymphoma with methotrexate and deferred radiotherapy: a report of NABTT 96-07. *J Clin Oncol* 21 (6): 1044-1049, 2003.
7) Pels H, Schmidt-Wolf IG, Glasmacher A, *et al*: Primary central nervous system lymphoma: results of a pilot and phase II study of systemic and intraventricular chemotherapy with deferred radiotherapy. *J Clin Oncol* 21 (24): 4489-4495, 2003.
8) Herrlinger U, Küker W, Uhl M, *et al*: NOA-03 trial of high-dose methotrexate in primary central nervous system lymphoma: final report. *Ann Neurol* 57 (6): 843-847, 2005.
9) Glass J, Gruber ML, Cher L, *et al*: Preirradiation methotrexate chemotherapy of primary central nervous sys-

tem lymphoma: long-term outcome. *J Neurosurg* **81**(2): 188-195, 1994.
10) O'Brien PC, Roos DE, Pratt G, *et al*: Combined-modality therapy for primary central nervous system lymphoma: long-term data from a Phase II multicenter study (Trans-Tasman Radiation Oncology Group). *Int J Radiat Oncol Biol Phys* **64**(2): 408-413, 2006.
11) Abrey LE, DeAngelis LM and Yahalom J: Long-term survival in primary CNS lymphoma. *J Clin Oncol* **16**(3): 859-863, 1998.
12) Blay JY, Bouhour D, Carrie C, *et al*: The C5R protocol: a regimen of high-dose chemotherapy and radiotherapy in primary cerebral non-Hodgkin's lymphoma of patients with no known cause of immunosuppression. *Blood* **86**(8): 2922-2929, 1995.
13) Bessell EM, López-Guillermo A, Villá S, *et al*: Importance of radiotherapy in the outcome of patients with primary CNS lymphoma: an analysis of the CHOD/BVAM regimen followed by two different radiotherapy treatment. *J Clin Oncol* **20**(1): 231-236, 2002.
14) Korfel A and Thiel E: Successful treatment of non-Hodgkin's lymphoma of the central nervous system with BMPD chemotherapy followed by radiotherapy. *Leuk Lymphoma* **30**(5-6): 609-617, 1998.
15) Brada M, Hjiyiannakis D, Hines F, *et al*: Short intensive primary chemotherapy and radiotherapy in sporadic primary CNS lymphoma (PCL). *Int J Radiat Oncol Biol Phys* **40**(5): 1157-1162, 1998.
16) Abrey LE, Yahalom J and DeAngelis LM: Treatment for primary CNS lymphoma: the next step. *J Clin Oncol* **18**(17): 3144-3150, 2000.
17) DeAngelis LM, Seiferheld W, Schold SC, *et al*: Combination chemotherapy and radiotherapy for primary central nervous system lymphoma: Radiation Therapy Oncology Group study 93-10. *J Clin Oncol* **20**(24): 4643-4648, 2002.
18) Poortmans PM, Kluin-Nelemans HC, Haaxma-Reiche H, *et al*: High-dose methotrexate-based chemotherapy followed by consolidating radiotherapy in non-AIDS-related primary central nervous system lymphoma: European Organization for Research and Treatment of Cancer Lymphoma Group Phase II Trial 20962. *J Clin Oncol* **21**(24): 4483-4488, 2003.
19) Ferreri AJ, Dell' Oro S, Foppoli M, *et al*: MATILDE regimen followed by radiotherapy is an active strategy against primary CNS lymphomas. *Neurology* **66**(9): 1435-1438, 2006.
20) Shah GD, Yahalom J, Correa DD, *et al*: Combined immunochemotherapy with reduced whole-brain radiotherapy for newly diagnosed primary CNS lymphoma. *J Clin Oncol* **25**(30): 4730-4735, 2007.
21) Ferreri AJ, Reni M, Foppoli M, *et al*: High-dose cytarabine plus high-dose methotrexate versus high-dose methotrexate alone in patients with primary CNS lymphoma: a randomized phase 2 trial. *Lancet* **374**(9700): 1512-1520, 2009.
22) Thiel E, Korfel A, Martus P, *et al*: High-dose methotrexate with or without whole brain radiotherapy for primary CNS lymphoma (G-PCNSL-SG-1): a phase 3, randomised, non-inferiority trial. *Lancet Oncol* **11**(11): 1036-1047, 2010.
23) Hiraga S, Arita N, Ohnishi T, *et al*: Rapid infusion of high-dose methotrexate resulting in enhanced penetration into cerebrospinal fluid and intensified tumor response in primary central nervous system lymphomas. *J Neurosurg* **91**(2): 221-230, 1999.
24) 泉本修一, 森 鏡二, 有田憲生: 悪性リンパ腫に対するHD-MTX療法の長期治療成績と問題点—多施設共同臨床研究から. 第26回日本脳腫瘍学会抄録集, 2008, p130.
25) Gerstner ER, Carson KA, Grossman SA, *et al*: Long-term outcome in PCNSL patients treated with high-dose methotrexate and deferred radiation. *Neurology* **70**(5): 401-402, 2008.
26) Illerhaus G, Marks R, Ihorst G, *et al*: High-dose chemotherapy with autologous stem-cell transplantation and hyperfractionated radiotherapy as first-line treatment of primary CNS lymphoma. *J Clin Oncol* **24**(24): 3865-3870, 2006.
27) Illerhaus G, Müller F, Feuerhake F, *et al*: High-dose chemotherapy and autologous stem-cell transplantation without consolidating radiotherapy as first-line treatment of primary lymphoma of the central nervous system. *Hematologica* **93**(1): 147-148, 2008.
28) Campen CJ, Tombleson RL and Green MR: High-dose chemotherapy with hemotopoietic stem cell transplantation for the treatment of primary central nervous system lymphoma. *J Neurooncol* **101**(3): 345-355, 2011.
29) Illerhaus G, Marks R, Müller F, *et al*: High-dose methotrexate combined with procarbazine and CCNU for primary CNS lymphoma in the elderly: results of a prospective pilot and phase II study. *Ann Oncol* **20**(2): 319-325, 2009.
30) Omuro AM, Taillandier L, Chinot O, *et al*: Temozolomide and methotrexate for primary central nervous system lymphoma in the elderly. *J Neurooncol* **85**(2): 207-211, 2007.
31) Fritsch K, Kasenda B, Hader C, *et al*: Immunochemotherapy with rituximab, methotrexate, procarbazine, and lomustine for primary CNS lymphoma (PCNSL) in the elderly. *Ann Oncol* **22**(9): 2080-2085, 2011.

Journal of Medicinal Chemistry

Brief Article

pubs.acs.org/jmc

Biological Evaluation of Dodecaborate-Containing L-Amino Acids for Boron Neutron Capture Therapy

Yoshihide Hattori,*[†] Shintaro Kusaka,[‡] Mari Mukumoto,[§] Kouki Uehara,[§] Tomoyuki Asano,[§] Minoru Suzuki,[∥] Shin-ichiro Masunaga,[∥] Koji Ono,[∥] Shinji Tanimori,[‡] and Mitsunori Kirihata[†]

[†]Research Center of Boron Neutron Capture Therapy, Research Organization for the 21st Century, Osaka Prefecture University, 1-1 Gakuen-cho, Nakaku 599-8531, Sakai, Japan

[‡]Department of Bioscience and Informatics, Graduate School of Life and Environmental Sciences, Osaka Prefecture University, 1-1 Gakuen-cho, Nakaku 599-8531, Sakai, Japan

[§]Stella Pharma Co., ORIX Kouraibashi Building 5F, 3-2-7 Kouraibashi, Chuo-ku, Osaka, Japan

[∥]Kyoto University Research Reactor Institute, 2 Asashiro-Nishi, Kumatori-cho, Sennan-gun, Osaka, Japan

ABSTRACT: To develop a boron carrier for practical purposes, new boron-containing amino acids with an undecahydro-*closo*-dodecaboranylthio ($[^{10}B_{12}H_{11}S]^{2-}$) unit in the side chain of the α-amino acid have already been designed and synthesized. In the present paper, cytotoxicity, the incorporation amounts into tumor cells, and the tumor cell killing effects of these compounds were elucidated to evaluate their usefulness as boron carriers. Furthermore, the microdistribution of the amino acids in tumor cells was established.

INTRODUCTION

Recently, boron neutron capture therapy (BNCT) has become recognized as an essential therapy for brain cancer, head and neck cancer, and melanoma.[1] BNCT is based on the nuclear capture and fission reactions of the ^{10}B atom with low energy thermal/epithermal neutrons to yield high linear energy transfer α particles and recoiling ^{7}Li nuclei. Because the path lengths of the articles are approximately 9−10 μm, equal to the dimensions of a single cell, ^{10}B-containing cells are selectively destroyed by BNCT.

Although many kinds of boron compounds, including amino acids, nucleic acids, and liposomes, have been reported as boron delivery agents (boron carriers) for BNCT,[2−6] only two compounds, *p*-borono-L-phenylalanine (BPA) and disodium mercapto-*closo*-undecahydrododecaborate ($[B_{12}H_{11}SH]^{2-}2Na^{+}$, BSH), are clinically used in treatment of cancer with BNCT.[7] For a boron delivery agent to be successful in BNCT, the compound must have following properties: (i) high tumor targeting selectivity ($T/N > 3-4:1$), (ii) low systemic toxicity, (iii) concentrations of ~20 μg ^{10}B/g tumor tissues, especially the boron compound, is preferred to accumulate into tumor cell and/or cell nuclei, and (iv) high water-solubility. On the other hand, the L-amino acid transport system in tumor cells is enhanced to ensure cell multiplication compared with normal tissues. Therefore, there has been a long-standing interest in the design, synthesis, and biological evaluation of boron-containing α-amino acids with tumor-seeking and tumor-localizing properties.

L-BPA has been used as an excellent boron delivery agent for BNCT. Because L-BPA is selectively uptaken into tumor cells, particularly accumulating in the cell nuclei, L-BPA is clinically used in BNCT.

BSH and its derivatives are of increasing interest as boron carriers for BNCT with the aim to deliver large amounts of ^{10}B atoms to tumor cells.[8] BSH is a class of water-soluble boron cluster compound and has low toxicity compared with another boron cluster compounds. Owing to these properties, BSH is clinically used for the treatment of brain tumors with BNCT as a ^{10}B carrier,[9] although tumor selectivity of BSH is slightly low.

To develop practical materials utilizing ^{10}B carriers, we previously designed and synthesized several new boron-containing amino acids, including C4-BSH-AA (n = 2) (**1a**), C5-BSH-AA (n = 3) (**1b**), and C8-BSH-AA (n = 6) (**1c**), which include the undecahydro-*closo*-dodecaboranylthio ($[^{10}B_{12}H_{11}S]^{2-}$) unit through a boron−sulfur−carbon bond connection to the side chain of α-amino acid[10] (Figure 1).

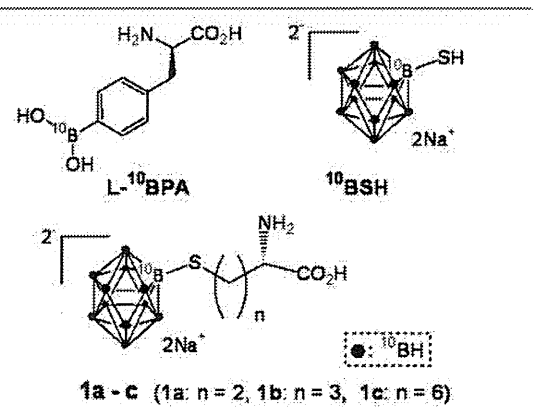

Figure 1. Boron-containing compounds.

Received: May 30, 2012
Published: July 12, 2012

Scheme 1. Synthesis of BSH-Amino Acids (1a–c)[a]

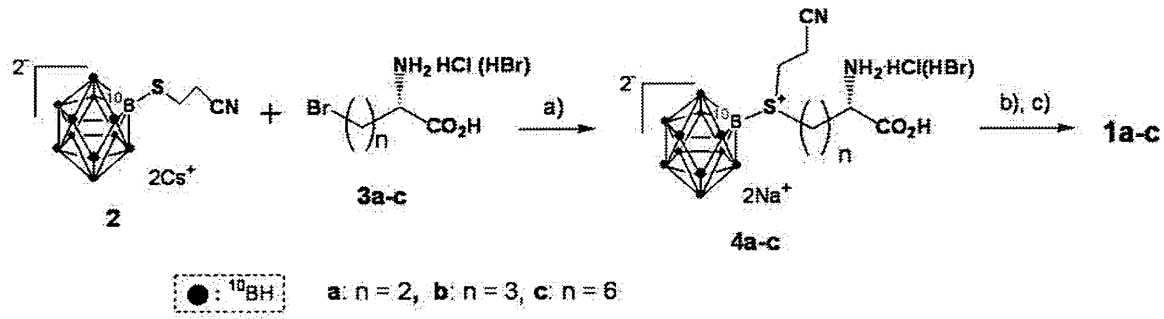

[a]Reagents and conditions: (a) MeCN, reflux, 24 h; (b) Me_4NOH, $MeNH_2$, acetone, rt, 30 min; (c) amberlite IR-120(Na^+).

Here, we report the distribution of the BSH-amino acids 1a–c in tumor cells and their cytotoxicities, the incorporated amount into cancer cells, and the tumor cell killing effects.

MATERIALS AND METHODS

General. L-^{10}BPA and ^{10}BSH were provided by Stella Pharma Corporation (Osaka, Japan). Capillary electrophoresis analysis was carried out using Photal CAPI-3300 (Otsuka Electronics Co. Ltd., Osaka, Japan) equipped with a fused silica capillary of 75 μm i.d. and a total length of 50 cm (effective length of 38 cm). A new capillary was conditioned with 0.1 M NaOH for 30 min followed by 15 min of distilled water and 15 min of electrolyte buffer (5 mM sodium phosphate buffer, pH 9.0). The applied potential was 20 kV and detection at 200 nm. Inductively coupled plasma optical emission spectrometry (ICP-OES) was obtained on a VISTA-MPX ICP-OES spectrometer (Seiko Instruments, Chiba, Japan). Fluor 488 goat anti-mouse IgG was purchased from Life Technologies (Carlsbad, CA, US). Permafluor was purchased from Immunotech (Marseille, France).

Synthesis of BSH-Amino Acids (1a, 1b, and 1c). The synthesis of BSH-amino acids 1a–c was carried out according to previously described method.[10] The purity of 1a–c was analyzed by capillary electrophoresis, and the analysis of 1a–c was revealed the purity to be >95%.

Cells and Cell Culture. SAS (human oral squamous cell carcinoma), B16 (mouse melanoma), and C6 (rat glioma) cell lines, used in cytotoxicity analyses, boron incorporation, tumor cell killing effect, and immunostaining, were cultured in Dulbecco's Modified Eagle's Medium (DMEM) supplemented with 10% fetal bovine serum (FBS), 2 mM glutamine, and 24 mM sodium hydrogen carbonate at 37 °C in a 5% CO_2 atmosphere. Cells in the monolayer were harvested with 0.25% trypsin/0.02% ethylenediaminetetraacetic acid (EDTA) in Ca^{2+}-free phosphate-buffered saline (PBS). Matrigel (growth factor reduced type) was purchased from BD Science (San Jose, CA, US).

Water-Soluble Tetrazolium (WST)-8 Assay. The cytotoxicity of each amino acid was assayed using the WST-8 assay with a cell counting kit (Wako Pure Chemicals, Osaka, Japan) following the manufacturer's protocols with some modifications. Briefly, a 96-well microplate was seeded with 5×10^3 cells suspended in 100 μL of cell growth media and allowed to settle for 16 h at 37 °C. The medium was removed by aspiration, and 100 μL of growth medium (DMEM with 10% FBS containing each compound at different concentrations) was added to each well. After incubation for 48 h at 37 °C, the medium was removed by aspiration and 100 μL of WST-8 solution [5 mM WST-8, 20 mM HEPES (pH 7.4) and 0.2 mM 1-methoxy PMS dissolved in PBS] were added to each well, followed by incubation for 4 h at 37 °C. The absorbance at 450 nm (reference: 655 nm) was read on a microwell plate reader. A well without cells was used as the blank. Relative cell survival was calculated as follows;

Table 1. Cytotoxicity of Boron Amino Acids against Tumor Cells

	IC_{50} (mM)		
compd	C6	SAS	B16
L-^{10}BPA	>2	>2	>2
C4-BSH-AA (1)	6.6	7.8	5.6
C5-BSH-AA (2)	2.4	4.9	6.6
C8-BSH-AA (3)	4.7	5.6	5.1

relative cell survival (%)
= (absorbance value of compound treated well
/absorbance value of untreated well) × 100

The relative cell survival was plotted against the compound concentration, and IC_{50} values for each compound were graphically determined.

Boron Incorporation into Cultured Tumor Cells. Cultures were inoculated with 1.0×10^6 cells/dish, and cells were grown for 24 h in DMEM. The medium was replaced with an equivalent medium containing each boron-containing amino acid (the final concentration was 2.0 mM in each case). The cells were cultured for 24 h, and the medium was then removed by aspiration. The cells were washed thrice with PBS, harvested by trypsinization, and then counted. Each sample, containing 1×10^6 cells, was added to a mixture of $HClO_4$ (60%, 0.3 mL) and H_2O_2 (31%, 0.6 mL) and then heated at 75 °C for 1 h. The mixture was filtered through a membrane filter (Millipore, 0.45 μm), and the boron concentration was measured by ICP-OES.

Immunostaining of C6 Cells. Immunostaining was performed to detemine the incorporation of boron-containing amino acids into C6 cells, according a previously described method with some modifications.[11] Glass coverslips coated with Matrigel (3.5 μg/cm^2 protein) were seeded with C6 cells (0.8×10^5 cells suspended in 3 mL of DMEM) and allowed to settle for 1 h at 37 °C. The medium was replaced with an equivalent medium containing compound 1a (the final concentration was 2.0 mM in each case), and the cells were cultured for 24 h at 37 °C. After being washed with DMEM, C6 cells were fixed with 10% paraformaldehyde in PBS for 10 min at room temperature. The cells were rinsed with PBS and treated with 0.05% Triton X-100 for 10 min at room temperature. Further, the cells were washed with PBS and preincubated in a humid chamber with 1.0% BSA/0.02% NaN_3 in PBS at room temperature, followed by incubation with the anti-BSH monoclonal antibody A9H3 in PBS containing 1.0% BSA/0.02% NaN_3 (0.2 μg/mL) for 60 min at 32 °C. The cells were rinsed with PBS and then incubated with Alexa-Fluor 488 goat anti-mouse IgG in PBS containing 1.0% BSA/0.02% NaN_3 (0.2 μg/mL) for 30 min at 32 °C. After washing with PBS, the cells were mounted with Permafluor and then photographed with a microscope (IX-70, Olympus, Tokyo) equipped with a cooled charge-coupled device

camera (UIC-QE, Molecular Devices Co., Sunnyvale, CA, U.S.) controlled by MetaMorph software (Molecular Devices Co.).

Tumor Cells Killing Effect Study. Cultures were inoculated with 1.0×10^6 cells/dish, and cells were grown for 24 h in DMEM. The medium was replaced with an equivalent medium containing each boron-containing amino acid (the final concentration was 2.0 mM in each case). They were cultured for 24 h, and the medium was removed by aspiration. The cells were washed with PBS, harvested by trypsinization, and then counted. After centrifugation, trypsin was removed by aspiration, and DMEM was added to the residual cells. The cell suspension in DMEM (5.0×10^3 cells/mL, 1 mL) was irradiated with thermal neutrons for 0–90 min in a column-shape tube. The thermal neutron fluence was determined by averaging two gold foils, symmetrically attached to the surface of the column-shape tube along the direction of incidence of the thermal neutrons. After thermal neutron exposure, 600 cells were placed in three Corning 60 mm tissue culture dishes containing 3 mL of DMEM to examine colony formation. Seven days later, the colonies were fixed with ethanol and stained with 0.1% crystal violet for quantitative visualization by the naked eye.

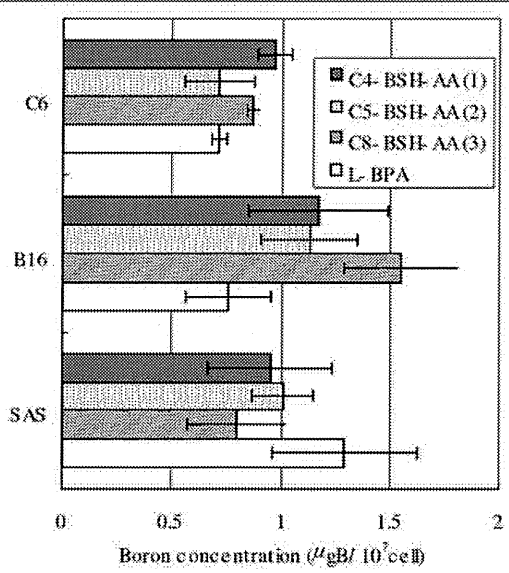

Figure 2. Incorporated amount of boron amino acids.

RESULTS AND DISCUSSION

An alternative route of synthesis of the three BSH-amino acids (**1a–c**) is illustrated in Scheme 1. As shown, the starting compound, *S*-(cyanoethyl)-BSH tetramethylammonium salt (**2**),[12] was prepared with a high yield by hetero-Michael reaction of BSH dicesium salt with acrylonitrile, using sodium hydroxide as a base.[13] On the other hand, the ω-bromo-L-amino acids (**3a–c**), represented as Br-$(CH_2)n$-CH(NH_2)-COOH (n = 2, 3, and 6, respectively), were prepared as hydrochloric or hydrobromic salts. Among these, (*S*)-2-amino-4-bromobutyric acid (**3a**, n = 2) was commercially purchased, and the others (**3b** and, **3c**) bearing the (*S*)-configuration were synthesized according to modified versions of published methods.[14,15]

The alkylation reaction of **2** with ω-bromo-L-amino acids (**3**) was completed by a simple procedure. The purity and chemical structure of **1** were analyzed by ^1H and ^{13}C NMRs, ESI-MS, and capillary electrophoresis. In the present synthesis, absolute configuration of the starting ω-bromo-L-amino acid was introduced to the final amino acids in retention without any racemization.

The cytotoxicities of the BSH-amino acids **1a–c** and L-BPA toward the C6, SAS, and B16 cell lines were determined using the WST-8 test (Table 1). As shown in Table 1, the cytotoxicity of each compound was very low. However, the cytotoxicity of the three BSH-amino acids was higher than that of L-BPA.

To elucidate the incorporation amounts of BSH-amino acids **1a–c** into cancer cells, we measured the boron concentrations in three kinds of cancer cells, C6, B16, and SAS by ICP-OES (Figure 1). The compounds **1a**, **1b**, and **1c** were up-taken into cancer cells. In particular, the amounts of **1a–c** that were incorporated ware higher than those of L-^{10}BPA for C6 and B16 cells. These results suggest that the BSH-amino acids **1a–c** are as useful as L-^{10}BPA as ^{10}B carrier.

To determine the distribution of each BSH-amino acid in tumor cells, we stained C6 cells that incorporated compound **1a** with the anti-BSH antibody A9H3[16] (Figure 2). The results showed the distribution of BSH-amino acid **1a** was very different from that of L-BPA. L-BPA was reported that widely distributed in the cytoplasm and the cell nuclei there are no regions within the cells in which the concentration of L-BPA is especially high.[17,18] In contrast, the compound **1a** was

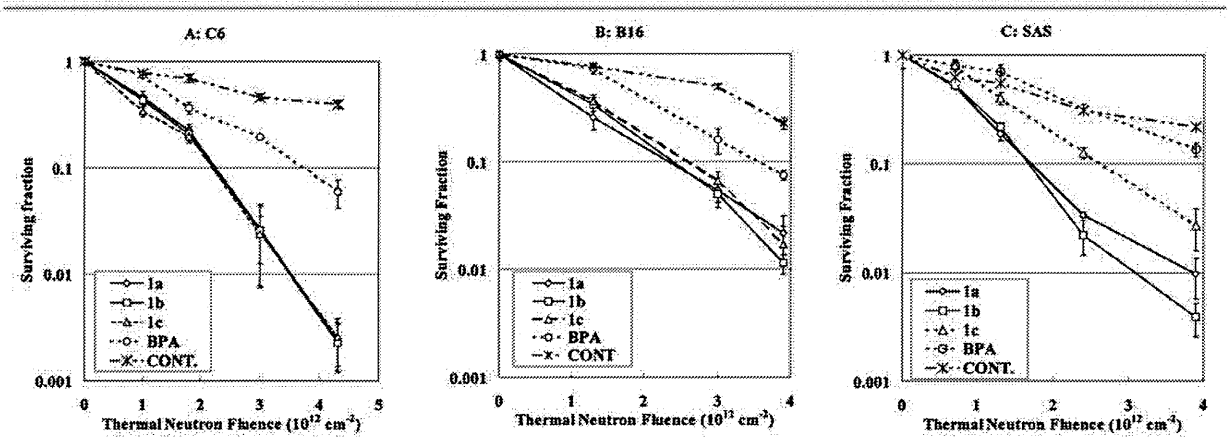

Figure 3. The tumor cell killing effects of boron-containing amino acids (A) against C6 cells, (B) against B16 cells, and (C) against SAS cells.

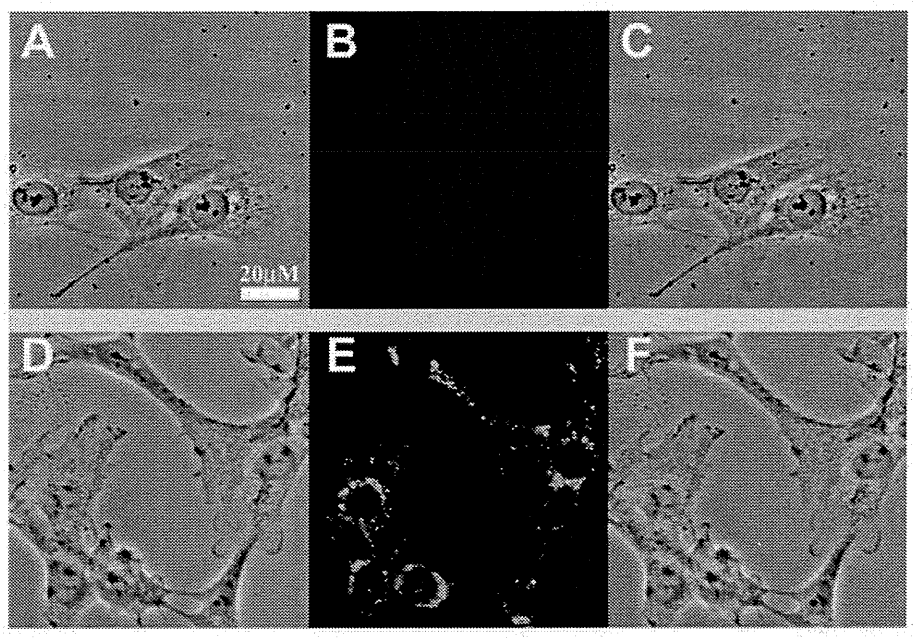

Figure 4. The microdistribution of compound 1a in C6 cells. (A) A phase-contrast micrograph of C6 cells that were cultured in DMEM. (B) A fluorescence micrograph of C6 cells that were cultured in DMEM stained with the anti-BSH antibody A9H3. (C) A merged image of A and B. (D) A phase-contrast micrograph of C6 cells that were cultured in DMEM containing compound 1a. (E) A fluorescence micrograph of C6 cells that were cultured in DMEM containing compound 1a stained with the anti-BSH antibody A9H3. (F) Merged image of D and E.

incorporated into the cell membrane of the C6 cells and aggregated on the fringe of the cell nuclei (Figure 4).

To confirm the usefulness of the BSH-amino acids 1a–c for BNCT, we examined the tumor cell killing effects of L-^{10}BPA and compounds 1a–c against tumor cells in vitro using neutron irradiation (Figure 3). Despite the finding that the amounts of the three amino acids incorporated were closely equivalent to that of L-^{10}BPA, 1a–c showed higher killing effects than L-^{10}BPA for all types of tumor cells tested.

■ CONCLUSION

From these results presented, we conclude that the undecahydro-*closo*-dodecaboranylthio unit is well suited as a boron source, and the BSH-amino acids 1a–c are useful as ^{10}B carriers because they aggregated on the fringe of the cell nuclei and showed higher cell-killing effects than L-BPA toward several tumor cells types. In vivo evaluation of compounds 1a–c is ongoing, and the results will be reported soon.

■ AUTHOR INFORMATION

Corresponding Author

*Phone: +81-72-254-8447. E-mail: y0shi_hattori@riast.osakafu-u.ac.jp.

Author Contributions

These authors contributed equally.

Notes

The authors declare no competing financial interest.

■ ACKNOWLEDGMENTS

We thank Professor K. Ogawa for his technical support with immunostaining.

■ ABBREVIATIONS USED

BNCT, boron neutron capture therapy; L-^{10}BPA, *p*-(^{10}B)-borono-L-phenylalanine; ^{10}BSH, mercapto-undeca-hydro-*closo*-dodeca(^{10}B)borate; ICP-OES, inductively coupled plasma optical emission spectrometry; WST, water-soluble tetrazolium; DMEM, Dulbecco's Modified Eagle's Medium; FBS, fetal bovine serum; HEPES, 4-(2-hydroxyethyl)-1-piperazineethanesulfonic acid

■ REFERENCES

(1) Barth, R. F.; Coderre, J. A.; Vicente, M. G.; Blue, T. E. Boron neutron capture therapy of cancer: current status and future prospects. *Clin. Cancer Res.* **2005**, *11*, 3987–4002.

(2) Soloway, A. H.; Tjarks, W.; Barnum, B. A.; Rong, F. G.; Barth, R. F.; Codogni, I. M.; Wilson, J. G. The chemistry of neutron capture therapy. *Chem. Rev.* **1998**, *98*, 1515–1562.

(3) Endou, H.; Kanai, Y. Amino acid transporter molecule as a drug target. *Nippon Yakugaku Zasshi* **1999**, *114*, 11–16.

(4) Kabalka, G. W.; Yao, M. The synthesis and use of boronated amino acids for boron neutron capture therapy. *Anti-Cancer Agents Med. Chem.* **2006**, *6*, 111–125.

(5) Srivastsva, R. R.; Shinghaus, R. R.; Kabalka, G. W. Synthesis of 1-amino-3-[2-(1,7-dicarba-*closo*-dodecaboran (12)-1-yl)ethyl]cyclo-butanecarboxylic acid: a potential BNCT agent. *J. Org. Chem.* **1997**, *62*, 4476–4478.

(6) Varadarajan, A.; Hawthorne, M. F. Novel carboranyl amino acids and peptides: reagents for antibody modification and subsequent neutron-capture studies. *Bioconjugate Chem.* **1991**, *2*, 242–253.

(7) Miyatake, S.; Tamura, Y.; Kawabata, S.; Iida, K; Kuroiwa, T.; Ono, K. Boron neutron capture therapy for malignant tumors related to meningiomas. *Neurosurgery* **2007**, *61*, 82–90.

(8) Slepukhina, I.; Gabel, D. Synthesis and in vitro toxicity of new dodecaborate-containing amino acids. Proceedings of 12th International Congress on Neutron Capture Therapy, Kagawa, Japan, October 9–13, 2006, pp 247–250.

(9) Kageji, T.; Mizubuci, Y.; Nagahiro, S.; Nakagawa, Y.; Kumada, H. Clinical results of boron neutron capture therapy (BNCT) for glioblastoma. *Appl. Radiat. Isot.* **2011**, *69*, 1823−1825.
(10) Kusaka, S.; Hattori, Y.; Uehara, K.; Asano, T.; Tanimori, S.; Kirihata, M. Synthesis of optically active dodecaborate-containing L-amino acids for BNCT. *Appl. Radiat. Isot.* **2011**, *69*, 1768−1770.
(11) Ogawa, K.; Wada, H.; Okada, N.; Harada, I.; Nakajima, T.; Pasquale, B. E.; Tsuyama, S. EphB2 and ephrin-B1 expressed in the adult kidney regulate the cytoarchitecture of medullay tubule cells through Rho family GTPases. *J. Cell Sci.* **2005**, *119*, 559−570.
(12) Gabel, D.; Moller, D.; Harfst, S.; Rosler, J.; Ketz, H. Synthesis of *S*-alkyl and *S*-acyl derivatives of mercaptoundeca-hydrododeca-borate, a possible boron carrier for neutron capture therapy. *Inorg. Chem.* **1993**, *32*, 2276−2278.
(13) Hattori, Y.; Uehara, K.; Asano, T.; Tanimori, S.; Kirihata, M. Synthesis of new derivatives by hetero-Michael addition in water. Proceedings of 14th International Congress on Neutron Capture Therapy, Buenos Aires, Argentina, October 25-29, 2010, pp 343−344.
(14) Kanai, F.; Isshiki, K.; Umezawa, Y.; Morishima, H.; Naganawa, H.; Takita, T.; Takeuchi, T.; Umezawa, H. Vanoxonin, A new inhibitor of thymidylate symyjetase. *J. Antibiot.* **1985**, *38*, 31−38.
(15) Watanabe, L. A.; Jose, B.; Kato, T.; Nishino, N.; Yoshida, M. Synthesis of L-α-amino-ω-bromoalkanoic acid for side chain modification. *Tetrahedron Lett.* **2004**, *45*, 491−494.
(16) Kirihata, M.; Uehara, K.; Asano, T.; Preparation of borocaptate-(10B) (BSH) derivatives as hapten compound for production of antibody against BSH. PCT Int. Appl. WO2007097065 A1 20070830, 2007.
(17) Chandra, S.; Kabalka, G. W.; Lorey, D. R.; Smith, D. R.; Coderre, J. A. Imaging of fluorine and boron from fuorinated boronophenylalanine in the same cell at organelle resolution by correlative ion microscopy and confocal laser scanning microscopy. *Clin. Cancer Res.* **2002**, *8*, 2675−2683.
(18) Wittig, A.; Arlinghaus, H. F.; Kriegeskotte, C.; Moss, R. L.; Appelman, K.; Schmid, K. W.; Sauerwein, W. A. G. Laser postionization secondary neutral mass spectrometry in tissue: a powerful tool for elemental and molecular imaging in the development of targeted drugs. *Mol. Cancer Ther.* **2008**, *7*, 1763−1771.

Peptide Science 2011; K. Sakaguchi (Ed.)
The Japanese Peptide Society (2012)

A Novel Modification Method of Peptides and Proteins by Anionic Dodecaborate Cage in Water

Yoshihide Hattori[1], Yuko Katsuta[1], Mari Mukumoto[1], Kouki Uehara[2], Youichirou Ohta[2], Tomoyuki Asano[2], Minoru Suzuki[3], Shin-ichiro Masunaga[3], Koji Ono[3], Shinji Tanimori[1], and Mitsunori Kirihata[1]

[1]Department of Bioscience and Informatics, Graduate School of Life and Environmental Sciences, Osaka Prefecture University, 1-1 Gakuen-cho, Nakaku, Sakai, Japan, [2]Stella Pharma Co., ORIX Kouraibashi Bldg. 5F, 3-2-7 Kouraibashi, Chuo-ku, Osaka, Japan, and [3]Kyoto University Research Reactor Institute, 2, Asashiro-Nishi, Kumatori-cho, Sennan-gun, Osaka, Japan
e-mail: y0shi_hattori@riast.osakafu-u.ac.jp

In order to conduct the thiododecaborate (-S-$[B_{12}H_{11}]^{2-}$) unit to the residual thiol groups on target peptides by coupling reaction under aqueous conditions, we have newly devised two modification reagents BSH-Npys (2) and BSH-DNpys (3). The synthesis of thiododecaborate-containing glutathione (4) and its analogues (5, 6) by use of 2 and 3, and biological evaluation in vitro as boron agent for BNCT were described.

Keywords: boron agent for BNCT, boron cage peptide, mercaptoundecahydro-*closo*-dodecaborate (BSH), thiododecaborate-containing peptide

Introduction

The boron cluster compounds comprised of anionic dodecaborate cage $[B_{12}H_{12}]^{2-}$ are particularly interesting molecule, because they have characteristic regular icosahedral structure and unique chemical and biological properties. Recently, many application studies of dodecaborate cage focused on their intrinsic properties are currently progressed in the various fields. One of the important applications of dodecaborate compounds is related to boron agent for boron neutron capture therapy (BNCT) for cancer. In particular, mercaptoundecahydro-*closo*-dodecaborate (BSH, $[B_{12}H_{12}]^{2-}SH$, **1**) in which boron atoms are enriched with ^{10}B isotope has been used clinically for the treatment of patients with malignant brain tumor by BNCT.

BNCT is based on the nuclear reaction of ^{10}B with thermal/epithermal neutrons to yield high linear energy transfer α particles (^4He) and recoiling ^7Li nuclei in tumor

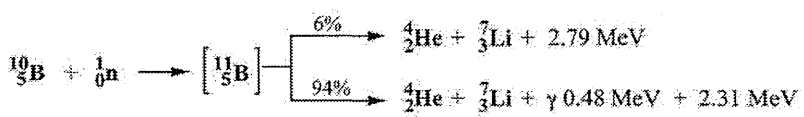

Fig. 1. Two Parallel Nuclear Fission between Neutron and ^{10}B Nucleus.

cells (Fig. 1) [1]. For a boron delivery agent to be successful in BNCT, the following criteria must be met: i) high tumor targeting selectivity (T/N >3-4:1); ii) low systemic toxicity; iii) tumor concentrations of ~ 20 μg ^{10}B /g tumor tissues. Over the past 20 years, various boron carrier molecules such as amino acids, nucleic acids and liposomes etc. have been designed and synthesized [2].

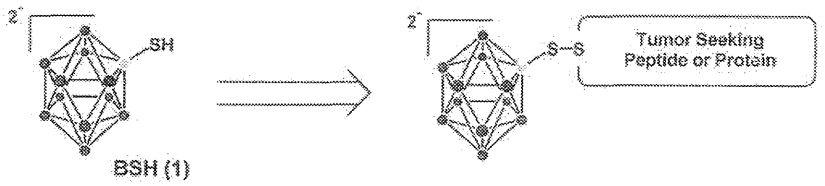

Fig. 2. Design Concept of Boron Agent for BNCT.

Our strategy for attaining the required concentration is to design the tumor seeking peptides or proteins such as antibodies bearing large number of polyhedral boron cages (Fig. 2). In the present study, we have adopted anionic thiododecaborate ($-S[B_{12}H_{12}]^{2-}$) unit linked to residual thiol groups on peptides or proteins by forming disulfide like (B-S-S-C) bonds, and also newly developed two modification reagents in order to conduct the unit to thiol groups.

We now described a new conjugation method of thiododecaborate unit to the thiol group on glutathione (GSH) and it's analogues used as a model peptide, and also their biological evaluation as boron agent for BNCT.

Results and Discussion

Preparation of Modification Reagents, BSH-Npys (2) and BSH-DNpys (3)

Two kinds of reagents (**2** and **3**) bearing nitropyridyl group for conjugation of thiododecabarate unit to thiol group were synthesized by the reaction of BSH2Cs with nitro/dinitro-pyridylsulfenyl chloride as pure state in moderate yield, respectively, as shown in Fig. 3.

Synthesis of Thiododecaborate-Containing Peptides (Thiododecaboration of Thiol Group)

The coupling reaction of GSH with **2** in aqueous solution was required long reaction time (over 3 days) to give GSH-BSH (**4**), and the isolation yield of disulfide **4** was slight low owing to by-production of GSH-dimer *in situ*. In contrast, the same coupling of GSH with **3** was furnished within 30 min to afford **4** in 81% isolation yield without any formation of BSH-dimer (Fig. 4). These results demonstrated BSH-DNpys **3** to be more suitable for the synthesis of thiododecaborate-contaning peptide. This reaction was applied to case of cystein-containing dipeptides, CysGly and CysVal, to give the corresponding CysGly-BSH (**5**) and CysVal-BSH (**6**), respectively, in good yield as shown in Fig. 5.

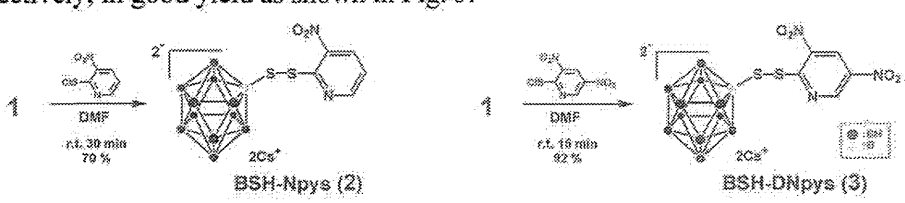

Fig. 3. Preparation of Modification Reagents 2 and 3.

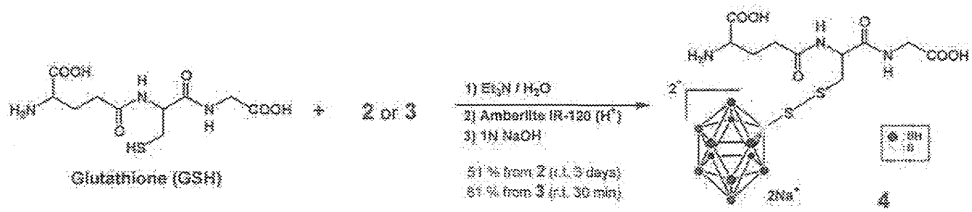

Fig. 4. Synthesis of Thiododecaborate-Containing GSH.

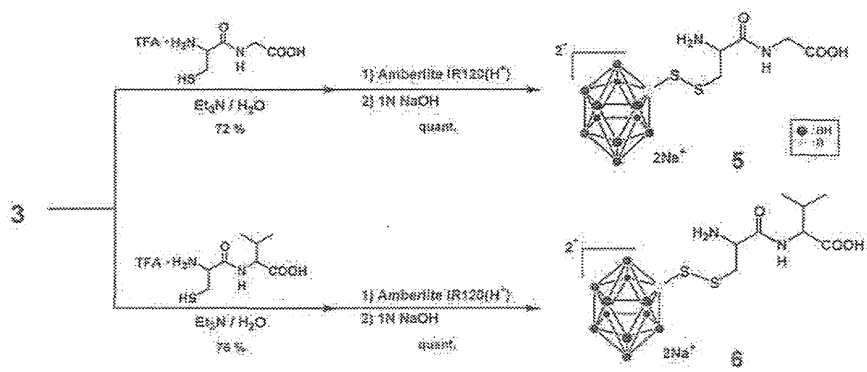

Fig. 5. Synthesis of Thiododecaborate-Containing Dipeptides.

Boron Uptake Study

To evaluate thiodecaborate-containing peptides **4-6** as boron agent for BNCT, we examined the boron uptake test using B16 (mouse melanoma) and C6 (mouse glioma) cells *in vitro*. The intracellular boron concentration was measured by inductively coupled plasma atomic emission spectroscopy (ICP-AES) technique. The boron concentrations of **4-6** in both cancer cells were higher than that of L-Boronophenylalanine (BPA) as of positive control substance, which was clinically used as boron agent in cure of cancer by BNCT (Fig. 5).

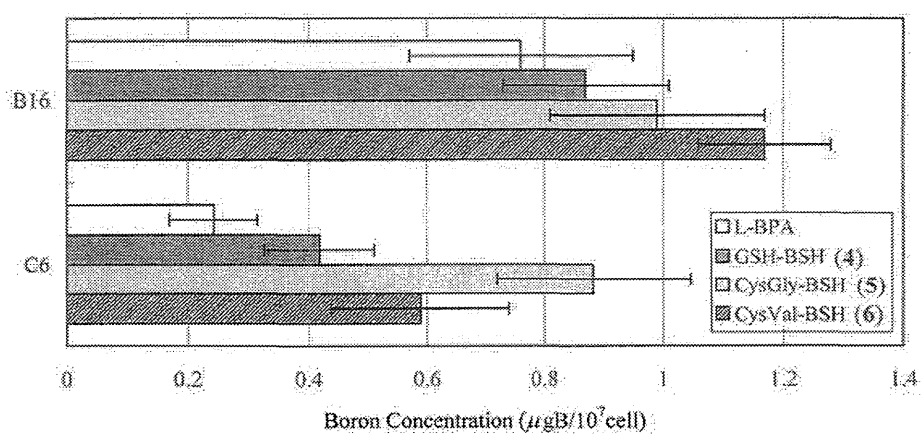

Fig. 6. Boron Concentration in B16 and C6 cells.

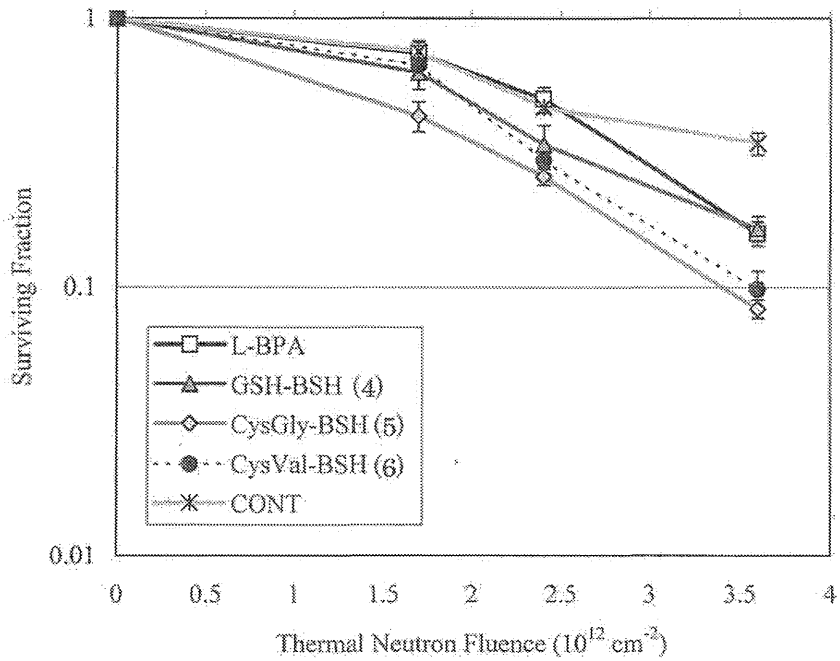

Fig. 7. Killing Effects by Neutron Irradiation Toward B16 Cell.

Killing Effect by Neutron Irradiation

Fig. 7 showed *in vitro* killing effects of peptides **4-6** toward B16 cell by neutron irradiation. Among these peptides, CysGly-BSH (**5**) showed the strongest killing effect in spite of its boron uptake was lower than **6**. Killing effects assay using another kind of cancer cell and mouse bearing cancer are currently in progress.

In conclusion, we accomplished the conductive method of thiododecaborate unit to the residual thiol groups on peptide in water by using of newly developed modification reagents, and also the biological activities of thiododecaborate-containing peptides synthesized here were evaluated. These thiododecaborate-containing peptides might be potentially useful in treating cancer by means of BNCT.

References

1. Barth, R. F.; Coderre, J. A.; Vicente, M. G.; Blue, T. E. (2005) *Cancer Res.*, **11**, 3987-4002.
2. Soloway, A. H.; Tjarks, W.; Barnum, B. A.; Rong, F. G.; Barth, R. F.; Codogni, I. M.; Wilson, J. G. (1998) *Chem. Rev.*, **98**, 1515–1562.

J Neurooncol (2011) 105:423–431
DOI 10.1007/s11060-011-0610-9

CLINICAL STUDY – PATIENT STUDY

The distribution of vascular endothelial growth factor-producing cells in clinical radiation necrosis of the brain: pathological consideration of their potential roles

Naosuke Nonoguchi · Shin-Ichi Miyatake · Motoi Fukumoto · Motomasa Furuse · Ryo Hiramatsu · Shinji Kawabata · Toshihiko Kuroiwa · Motomu Tsuji · Manabu Fukumoto · Koji Ono

Received: 21 January 2011 / Accepted: 22 May 2011 / Published online: 18 June 2011

Abstract The cell type and localization of vascular endothelial growth factor (VEGF)-producing cells in human radiation necrosis (RN) are investigated from a histopathological and immunohistochemical standpoint using clinical specimens. Eighteen surgical specimens of symptomatic RN in the brain were retrospectively reviewed. These cases included different original histological tumor types and were treated with different radiation modalities. Histological analyses were performed using hematoxylin and eosin (H&E) staining, and anti-VEGF and anti-hypoxia-inducible factor (HIF)-1α immunohistochemistry. H&E staining showed marked angiogenesis and reactive astrocytosis at the perinecrotic area. The most prominent vasculature in this area was identified as telangiectasis. Immunohistochemistry indicated that HIF-1α was expressed predominantly in the perinecrotic area and that a large majority of VEGF-expressing cells were reactive astrocytes intensively distributed in this area. VEGF produced by the reactive astrocytes localized mainly in the perinecrotic area might be a major cause of both angiogenesis and the subsequent perilesional edema typically found in RN of the brain. The benefits of anti-VEGF antibody (bevacizumab) treatment in RN may be that VEGF secretion from the perinecrotic tissue is inhibited and that surgery would remove this tissue; both of these benefits result in effective reduction of edema associated with RN.

Keywords Angiogenesis · Bevacizumab · Boron neutron capture therapy · Hypoxia-inducible factor-1α · Radiation necrosis · Vascular endothelial growth factor

Introduction

White matter necrosis, demyelination, and vascular damage in the central nervous system (CNS) are the major dose-limiting side-effects in radiation therapy, not only for intracranial neoplasms but also for neoplasms of the head and neck region.

Histopathologically, the changes in vasculatures associated with radiation necrosis (RN) are largely degenerative or dystrophic, and feature telangiectasis, hyaline thickening of vessels, and fibrinoid necrosis with intravascular thromboses. Pathophysiologically, RN is characterized by increased permeability and disruption of the blood–brain barrier [1]. It is thought that such radiation vasculopathy may account for sporadic focal ischemia and/or microbleeding, and that, in later stages (weeks to years after radiation exposure), it may lead to a progressive mass effect with severe perilesional edema that can result in

Electronic supplementary material The online version of this article (doi:10.1007/s11060-011-0610-9) contains supplementary material, which is available to authorized users.

N. Nonoguchi · S.-I. Miyatake (✉) · M. Furuse · R. Hiramatsu · S. Kawabata · T. Kuroiwa
Department of Neurosurgery, Osaka Medical College, Takatsuki, Japan
e-mail: neu070@poh.osaka-med.ac.jp

M. Fukumoto · M. Fukumoto
Department of Pathology, Institute of Development, Aging and Cancer, Tohoku University, Sendai, Japan

M. Tsuji
Department of Clinical Pathology, Osaka Medical College, Takatsuki, Japan

K. Ono
Particle Radiation Oncology Research Center, Research Reactor Institute, Kyoto University, Kumatori, Japan

aggravation of symptoms in patients. Thus, the delayed necrosis of the brain following exposure to high doses of radiation should be recognized as a hazard.

New radiation therapies with high absorbed doses within tumor tissue, such as intensity-modulated radiation therapy, particle radiation therapy, and boron neutron capture therapy (BNCT), have recently been used to treat patients with malignant brain tumors, including glioblastoma (GB). High-dose radiation treatments may have potential for greater rates of tumor control [2–6], but this is typically at the expense of greater rates of RN within the treatment volume. Also, stereotactic radiosurgery (SRS) achieves good control over metastatic brain tumors with the risk of RN [7]. Medical therapy is often started first and surgery reserved for use only if the lesion is refractory, unless there is an increase in symptomatic intracranial pressure [8, 9]. In some cases, however, removal of only the center of the necrotic core does not result in rapid shrinkage of edema (personal experience and data not shown). Recently, bevacizumab, an anti-vascular endothelial growth factor (VEGF) antibody, has been recognized as a novel potential tool for treatment of RN [10–12], as we also reported [13]. This allowed us to understand the primary factors in the critical exacerbation of RN. However, it has been unclear what kinds of cells mainly produce and secrete VEGF as a target of bevacizumab or where the VEGF-producing cells exist in the brain with symptomatic RN. Thus, no report has clearly described the extent of surgical resection that is necessary and sufficient to educe the maximal therapeutic effect of surgical resection of necrotic tissue.

To identify the origin of VEGF in RN and to obtain answers to the questions above, we retrospectively reviewed clinical specimens of symptomatic RN by hematoxylin and eosin (H&E) staining and immunohistological analyses of VEGF and hypoxia-inducible factor (HIF)-1α, especially from the standpoint of the occurrence of angiogenesis and perilesional edema in RN. We also summarize the results of surgical treatment and bevacizumab treatment for symptomatic RN.

Patients and methods

Patients

From June 2004 to December 2009, a total of 27 symptomatic RN cases was treated at Osaka Medical College (Table 1). In this period, a total of 27 symptomatic RN cases were treated at this institute. They were treated mainly by S.-I.M., and were followed up for at least 1 month with medical treatment, including mainly oral steroids, anticoagulants, vitamin E, and others. Pathological examination of the original tumor revealed various histological types, including GB, metastatic brain tumor, and malignant meningioma, and also head and neck cancer. All patients were treated with intensive radiation therapy including proton particle radiation, SRS or tumor-targeting particle radiation (BNCT) [5, 14] with or without fractionated X-ray treatment. Table 1 lists the use of preceding radiotherapy in recurrent cases and chemotherapeutic agents just prior to onset of symptomatic RN.

Preoperative diagnosis of RN was performed by fluoride-18-labeled boronophenylalanine positron emission tomography (F-BPA-PET), as reported previously [14, 15]. Even if PET analysis suggested the lesion was RN, it did not exclude the possibility that a small quantity of living tumor cells remained in or around the lesion. In other words, PET determination as RN means that RN should be the major cause of radiographic enhancement and perilesional edema. For cases 1–18, the MRI-enhanced area was surgically excised with the aid of 5-aminolevulinic acid (ALA) [16, 17]. All 18 cases showed massive necrosis on H&E staining, which proved that PET as described above accurately diagnosed RN. All other cases (cases 19–27) received only conservative medical treatment. Six recent cases (cases 16, 23–27) were treated with bevacizumab. In one of these cases, necrotic foci were surgically excised initially and treated again with bevacizumab when recurrence of RN was observed (case 16). All patients were followed up with periodic computed tomography (CT) or magnetic resonance imaging (MRI). Neuroimaging revealed intralesional or perilesional bleeding in four cases (cases 8, 13, 20, and 22).

Histological and immunohistological analyses

Specimens from 18 cases with surgically removed necrotic masses underwent histological examination. Of the 18 surgical specimens that had sufficient volume for immunohistological analyses, 11 were preserved and analyzed for VEGF expression using anti-VEGF antibody (1:200 dilution; A-20; Santa Cruz Biotechnology, Santa Cruz, CA). Briefly, sections were deparaffinized and nonspecific binding was blocked with 1% nonfat milk and 0.1% Triton X. Immunohistochemistry was performed in an automatic stainer using the I-VIEW DAB universal kit according to the manufacturer's protocol (Ventana Medical Systems, Tucson, AZ, USA).

In addition, anti-HIF-1α (1:50 dilution; monoclonal mouse anti-human HIF-1α, clone H1alpha67; Novus Biologicals, Littleton, CO, USA) immunohistological analysis was applied in these 11 cases.

Table 1 Patient profile of symptomatic radiation necrosis

Case	Age (years)	Gender	KPS[a] (preop.)	KPS[b] (postop.)	Original dis.	Radiation[c]	Duration[d]	Steroids[e]	Chemotherapy
Surgical cases (excision for enhanced area on MRI)									
Case 1[f]	78	M	70	90	Sal. Duc. Ca.	XRT (NA), BNCT ×2 (6.1, 10.1 Gy-Eq)	20	4→0	–
Case 2[g]	73	F	60	60	GB	XRT (60 Gy), BNCT (11.7 Gy-Eq)	3	3→1	ACNU
Case 3	48	M	50	40	GB	SRS (20 Gy), BNCT (12.4 Gy-Eq)	12	8→1	ACNU, TMZ
Case 4	64	F	60	80	GB	BNCT (9.7 Gy-Eq), XRT (30 Gy)	12	4→0	–
Case 5	40	F	50	50	GB	BNCT (15.7 Gy-Eq), XRT (50 Gy)	8	2→0	TMZ
Case 6	57	M	50	70	GB	XRT (60 Gy), BNCT (13.6 Gy-Eq)	8	8→2	ACNU
Case 7	73	F	80	80	GB	BNCT (13.1 Gy-Eq), XRT (30 Gy)	8	2→0	–
Case 8[i]	42	M	60	70	GB	SRS (20 Gy), XRT (63 Gy)	8	4→2	ACNU
Case 9	57	F	70	80	Metastasis (Ade. Ca.)	SRS (22 Gy)	9	4→0	Herceptin
Case 10	28	F	60	60	MM	SRS ×2 (20, 15 Gy), BNCT ×2 (10.1, 10.2 Gy-Eq)	12	4→2	–
Case 11	61	F	60	60	MM	SRS (40 Gy), BNCT (8.7 Gy-Eq)	8	2→2	–
Case 12	23	F	60	60	GB	BNCT (10.8 Gy-Eq), XRT (50 Gy)	16	4→2	–
Case 13[i]	48	M	60	40	GB	XRT (60 Gy), BNCT (13.7 Gy-Eq)	5	5→4	PCV
Case 14	42	M	60	60	GB	XRT (60 Gy), BNCT (12.7 Gy-Eq)	5	4→4	PCV
Case 15	26	F	80	90	GB	BNCT (12.6 Gy-Eq), XRT (30 Gy)	14	4→2	–
Case 16[h]	53	F	70	80	GB	Proton (50 Gy-Eq), XRT (40 Gy)	5	4→1	ACNU
Case 17[f]	47	F	80	90	Ade. Ca.	XRT (NA), BNCT ×2 (NA)	7	6→0	–
Case 18	55	M	90	90	Metastasis (Ade. Ca.)	XRT (30 Gy), SRS (18 Gy)	11	4→0	–
Nonsurgical cases (treated medically)									
Case 19[f]	72	F	60	90	Ade. Ca.	XRT (NA), BNCT ×4 (NA)	6	2→0	–
Case 20[i]	58	F	90	100	GB	BNCT (11.5 Gy-Eq), XRT (40 Gy)	5	2→0	TMZ
Case 21	37	F	80	90	AA	XRT (50 Gy), SRS (10 Gy)	5	6→1	TMZ
Case 22[i]	73	M	90	70	GB	BNCT (12.2 Gy-Eq), XRT (30 Gy),	6	2→2	TMZ
Case 23[h]	58	F	50	80	Metastasis (LC Ade. Ca.)	XRT (30 Gy), SRS (30 Gy)	6	4→0	–
Case 24[h]	39	M	90	100	GB	BNCT (11.9 Gy-Eq), XRT (20 Gy)	10	4→0	TMZ
Case 25[h]	56	F	60	60	MM	XRT (50 Gy), SRS (32 Gy), BNCT (12.5 Gy-Eq)	12	2→2	–
Case 26	74	F	70	70	Metastasis (LC Ade. Ca.)	SRS (22 Gy)	24	4→0	–
Case 27[h]	55	M	80	90	Metastasis (LC small)	SRS (22.5 Gy)	18	1→0	CDDP, VP-16

ACNU nimustin, *TMZ* temozolomide, *PCV* procarbazine, nimustin, vincristin, *AA* anaplastic astrocytoma, *CDDP* cisplatinum, *VP-16* etoposide, *dis* disease

[a] *KPS* Karnofsky performance score assessed just prior to the treatment

[b] *KPS* Karnofsky performance score assessed at 1 month after the initiation of the treatment

[c] *XRT* X-ray treatment, *BNCT* boron neutron capture therapy, *SRS* stereotactic radiosurgery, *Gy-Eq* biologically equivalent X-ray dose that would have equivalent effects on tumor and on normal brain. In BNCT, the presented dose is the peak point dose for normal brain. The method to estimate this dose was described in detail previously in references [4] and [10]. In SRS, the presented dose is marginal X-ray or gamma-ray dose. *NA* not available

[d] Months between termination of last radiotherapy and onset of symptoms caused by radiation necrosis

[e] Amounts of betamethasone (mg/day) just prior to the treatment and 1 month after the initiation of the treatment

[f] Head and neck cancer, RN occurred in the brain parenchyma

[g] S/O pseudoprogression

Sal. Duc. Ca. salivary ductal carcinoma, *GB* glioblastoma, *Ade. Ca.* adenocarcinoma, *MM* malignant meningioma, *LC* lung cancer, *small* small cell carcinoma

[h] Bevacizumab-treated

[i] Intracerebral hemorrhage on magnetic resonance imaging (MRI)

Results

Histological analysis with H&E staining

Two representative cases of surgically excised necrotic tissue are presented in Fig. 1 (cases 9, 13). Among the 18 surgically treated cases, these 2 cases were selected for presentation because their original tumor histologies and/or treatment radiation modalities differed as shown in Table 1 and because they were expected to reveal common and universal findings in human RN. Typical pathological changes were observed with H&E staining at the border zone between the completely necrotic areas and the normal brain areas, which we term the "perinecrotic" area. The most characteristic vasculature had an enlarged lumen composed of a thin wall with a single layer of endothelial cells that mimics capillaries; this condition is described as telangiectasis. In addition, other typical pathological changes, such as microscopic bleeding, were frequently observed (Fig. 1a). In some specimens, proliferation of arterioles was also observed (data not shown). Characteristic telangiectasis was observed in all of the surgically excised necrotic tissues, irrespective of the original tumor histological type and radiation modality, as listed in Table 1 (cases 1–18). Furthermore, hyalinization or fibrinoid necrosis of the vessels was commonly found in the perinecrotic area (data not shown).

Immunohistological analysis with anti-VEGF antibody

In immunohistological analysis using anti-VEGF antibody (Figs. 2, 3), almost all astrocytes in the perinecrotic area were strongly positive for VEGF expression. This was confirmed by double staining of anti-VEGF and anti-GFAP antibody (Fig. S1). Interestingly, there was little or no expression of VEGF in the necrotic core or in the undamaged brain tissue around the necrosis (Fig. 2). These VEGF-positive astrocytes were identified as reactive astrocytes morphologically and immunohistologically, as above. They were localized only within a few millimeters from each necrotic core. Outside of this very narrow marginal zone, the number of VEGF-expressing cells decreased dramatically in all specimens. A representative VEGF expression pattern is depicted in Fig. 3. Typical angiogenesis, namely telangiectasis, was observed in the perinecrotic area where abundant expression of VEGF was concomitantly observed (Fig. 3). In the other six samples from different patients who had undergone immunohistological analyses, the same features were found with regard to VEGF expression as described above (data not shown).

Another characteristic finding was endothelial proliferation, which is composed of stratified and swollen endothelial cells and typically recognized in GB prior to radiotherapy. In our series, this endothelial proliferation was observed in RN in GB as well as in RN in malignant

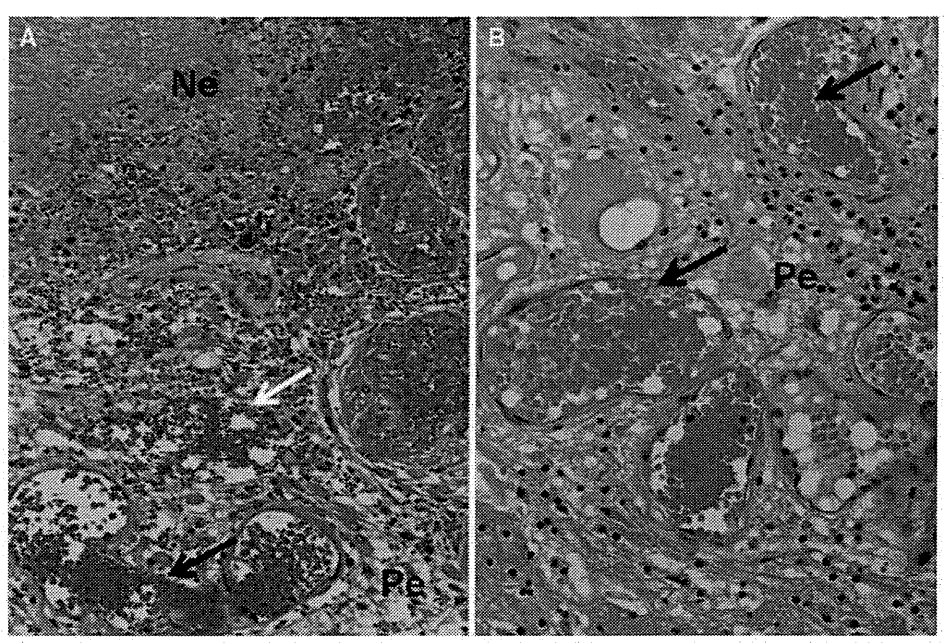

Fig. 1 Typical H&E staining of the surgical specimens from cases 9 and 13. **a** Case 13, RN derived from GB caused by XRT and BNCT. **b** Case 9, RN derived from metastatic brain tumor caused by SRS. In **a** and **b**, *black arrows* indicate telangiectasis and a *white arrow* shows bleeding in the interstitial space. *Ne* necrotic center, *Pe* perinecrotic area. In **a** and **b**, original objective magnification ×20 and ×40, respectively

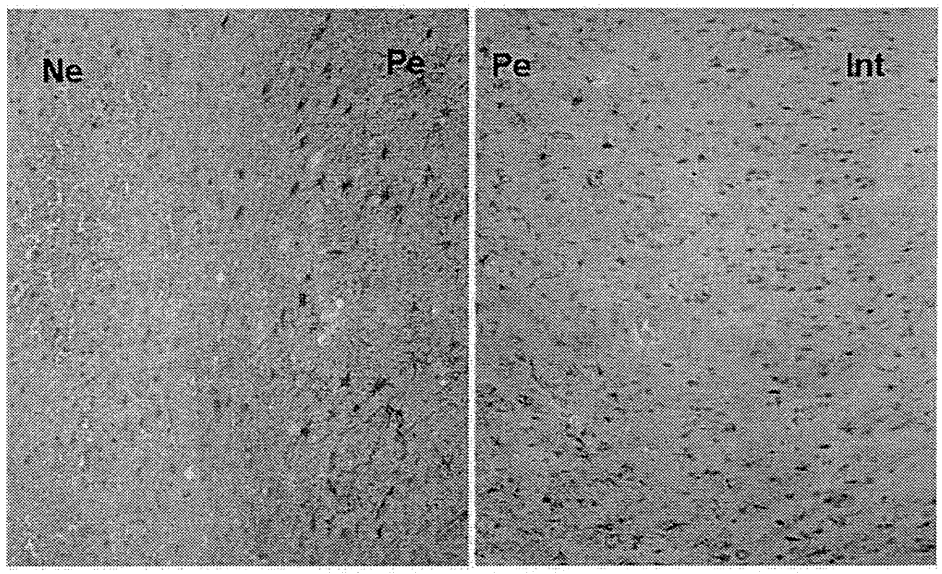

Fig. 2 Immunohistochemistry for VEGF of the surgical specimen from case 13. Many astrocyte-like cells in the perinecrotic area were strongly positive for VEGF expression. On the other hand, little or no immunoreactivity of VEGF was observed in the necrotic center or intact brain area. *Ne* necrotic center, *Pe* perinecrotic area, *Int* intact brain. Original objective magnification ×20

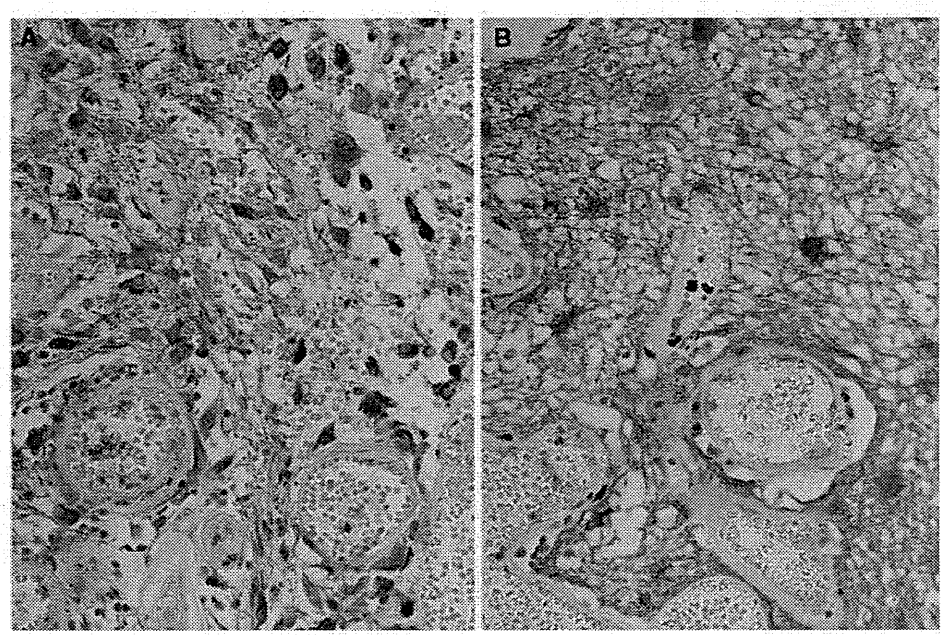

Fig. 3 Immunohistochemistry for VEGF of the perinecrotic area from cases 9 and 13. **a** and **b** are the same specimens depicted in Fig. 1. Strong immunoreactivity for VEGF and angiogenesis was observed in the perinecrotic area in **a** and **b**. Original objective magnification ×40

meningioma (data not shown), and even in the RN of the brain associated with radiotherapy for head and neck malignancies (cases 1 and 17, data not shown). It is noteworthy that the cells in endothelial proliferation and the endothelial cells in wall telangiectasis showed weaker intensity of immunoreactivity for VEGF and fewer cells, in comparison with the VEGF-positive astrocytes in the perinecrotic area (data not shown). Endothelial proliferation in the perinecrotic area was surrounded by a lot of VEGF-positive reactive astrocytes with no evidence of obvious tumor cell proliferation. It is difficult to deny completely that these endothelial proliferations derived and survived from tumor tissue after radiotherapy, especially in GB cases. However, this endothelial proliferation was also observed even in RN in the brains of head and neck cancer patients whose brains had no tumor cells. This strongly suggested that these endothelial proliferations were stimulated by the pathological signals, including VEGF, produced in the perinecrotic area.

Immunohistological analysis with anti-HIF-1α antibody

In Fig. S2, representative HIF-1α expression is depicted from three cases (cases 13, 16, and 17). HIF-1α was

strongly expressed in the cells in the perinecrotic area. At a glance, these cells look like gemistocytic astrocytes. On the other hand, little expression was observed in undamaged brain (Fig. S2A) or in the necrotic center (Fig. S2C). This tendency of HIF-1α expression was confirmed in all five of the other surgical cases examined.

Effectiveness of surgical and medical treatments for radiation necrosis

Typical rapid shrinkage of the perilesional edema in surgical treatment cases is shown in Fig. 4. Also, all patients treated with bevacizumab showed reduced perilesional edema. One example is shown in Fig. S3. The necessary amounts of steroid were reduced in 16 out of 18 surgically treated cases (88.9%) and in 7 out of 9 medically treated cases (77.8%), for a total of 23 out of 27 cases (85.2%). The Karnofsky performance score (KPS) improved in 13 out of 27 cases (50.6%). However, 3 of the 18 surgically treated cases and 1 of the 9 medically treated cases showed deterioration in KPS (Table 1).

Discussion

Several cytokines and chemokines such as VEGF, platelet-derived growth factor, and histamine can modulate vascular permeability, but single blockade of VEGF by an anti-VEGF antibody can significantly reduce the perifocal edema associated with RN in clinical cases. This result demonstrates that VEGF is one of the major permeability factors in human RN and plays a key role in its pathophysiology.

VEGF has two important biological properties. One is a strong angiogenic peptide component [18, 19], and the other is as a vascular permeability factor [20, 21]. In clinical RN, the former function may produce telangiectasis as pathological angiogenesis, and the latter function

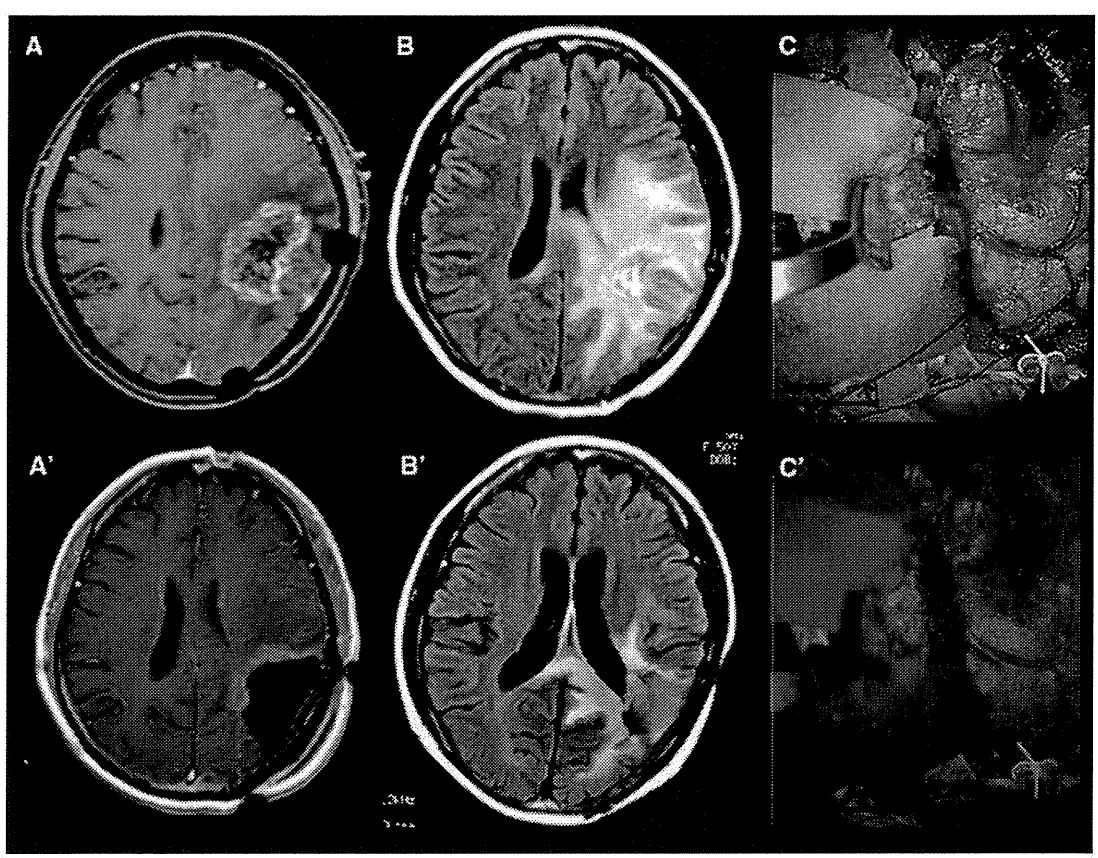

Fig. 4 Periodic changes in neuroimaging and intraoperative photographs of case 16. **a** Gd-enhanced T1 MRI just prior to excision of necrotic foci. **a'** Gd-enhanced T1 MRI 24 h after surgery. **b** FLAIR MRI just prior to excision of necrotic foci. **b'** FLAIR MRI, 1 month after surgery. Perilesional edema was decreased compared with preoperative MRI. **c** Intraoperative photograph under bright field demonstrating dissection of perinecrotic tissue from the surrounding brain. **c'** Intraoperative photograph under dark field with excitation for red fluorescence of protoporphyrin IX. *Red fluorescence* shows the perinecrotic area